Atmos. Chem. Phys., 7, 5873–5881, 2007
www.atmos-chem-phys.net/7/5873/2007/

Atmospheric Chemistry and Physics

Atmospheric deuterium fractionation: HCHO and HCDO yields in the $CH_2DO + O_2$ reaction

E. J. K. Nilsson[1], M. S. Johnson[1], F. Taketani[2], Y. Matsumi[2], M. D. Hurley[3], and T. J. Wallington[3]

[1]Copenhagen Center for Atmospheric Research, Department of Chemistry, University of Copenhagen, Universitetsparken 5, 2100 Copenhagen Ø, Denmark
[2]Solar-Terrestrial Environment Laboratory and Graduate School of Science, Nagoya University 3-13 Hohohara, Toyokawa, Aichi 442-8507, Japan
[3]Research and Innovation Center, Ford Motor Company, Dearborn MI 48121-2053, USA

Received: 14 May 2007 – Published in Atmos. Chem. Phys. Discuss.: 11 July 2007
Revised: 4 October 2007 – Accepted: 7 November 2007 – Published: 27 November 2007

Abstract. The formation of formaldehyde via hydrogen atom transfer from the methoxy radical to molecular oxygen is a key step in the atmospheric photochemical oxidation of methane, and in the propagation of deuterium from methane to molecular hydrogen. We report the results of the first investigation of the branching ratio for HCHO and HCDO formation in the $CH_2DO + O_2$ reaction. Labeled methoxy radicals (CH_2DO) were generated in a photochemical reactor by photolysis of CH_2DONO. HCHO and HCDO concentrations were measured using FTIR spectroscopy. Significant deuterium enrichment was seen in the formaldehyde product, from which we derive a branching ratio of 88.2±1.1% for HCDO and 11.8±1.1% for HCHO. The implications of this fractionation on the propagation of deuterium in the atmosphere are discussed.

1 Introduction

Changes in atmospheric chemistry during the Anthropocene are linked to perturbations to the carbon cycle (IPCC, 2001; Wang and Jacob, 1998), documented in part by isotopic analysis. The goal of the present work is to determine how deuterium propagates through the $CH_3O + O_2$ reaction which is a key step in the atmospheric oxidation of methane (Feilberg et al., 2005b, 2007; Keppler et al., 2006; Quay et al., 1999; Rockmann et al., 2002; Saueressig et al., 2001; Weston, 2001):

$$CH_4 \rightarrow CH_3 \rightarrow CH_3O_2 \rightarrow CH_3O \rightarrow HCHO \rightarrow CO \rightarrow CO_2$$

An overview of the reaction system is shown in Fig. 1. Knowledge of the isotopic signatures of the specific steps can be used to reduce uncertainties regarding the sources and sinks of the trace gases involved. Formaldehyde is a key intermediate in the oxidation of methane and non-methane hydrocarbons (in particular isoprene) (Hak et al., 2005; Palmer et al., 2006). The photolysis of formaldehyde is the only important in-situ source of molecular hydrogen in the atmosphere; at present about half of atmospheric H_2 is produced in this way (Gerst and Quay, 2001). There is interest in using hydrogen as an energy carrier replacing conventional hydrocarbon fuels. Potential advantages include reductions in CO_2, NOx and hydrocarbon emissions. Potential impacts associated with leaks from storage and distribution systems are modest and include small increases in stratospheric water vapor and additional consumption of OH (that would otherwise react with CH_4) and implying a small effect on greenhouse gas budgets (Prather, 2003; Schultz et al., 2003). There are significant uncertainties in our knowledge of the hydrogen budget (IPCC, 2001; Quay et al., 1999; Rhee et al., 2006b).

The present atmosphere is the foundation for predicting future trends in greenhouse gas emissions. Uncertainties concerning the sources and sinks of greenhouse gases have been identified by the IPCC as a significant obstacle to accurately predicting future climate change (IPCC, 2001). Isotopic analysis is an important tool for investigating sources and loss mechanisms for atmospheric trace gases (Brenninkmeijer et al., 2003; Johnson et al., 2002). Examples include understanding ice core records of injection of sulfur into the stratosphere (Baroni, 2007), quantifying terrestrial CO_2 sinks (Miller et al., 2003), refining the nitrous oxide budget (von Hessberg et al., 2004) and identifying the missing source of atmospheric methyl chloride (Gola et al., 2005; Keppler et al., 2005). Two key sources of atmospheric hydrogen, fossil fuel combustion and biomass burning, are depleted in D, having $\delta D(H_2)$ values of -196 ± 10‰ and

Correspondence to: M. S. Johnson
(msj@kiku.dk)

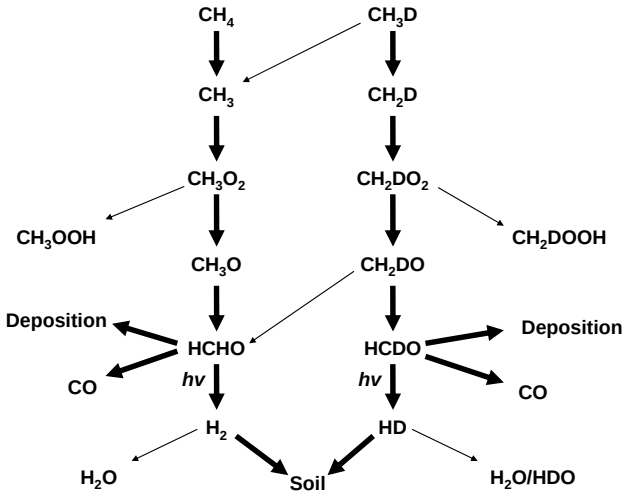

Fig. 1. Propagation of deuterium through gas-phase atmospheric reactions converting methane to hydrogen. Co-reagent species are omitted for clarity, for full reaction mechanism see Table 1.

-290 ± 60‰ respectively (Gerst and Quay, 2001). The processes removing molecular hydrogen from the atmosphere, soil uptake and OH reaction, are slower for HD than for HH by factors of 0.943 ± 0.024 (Gerst and Quay, 2001) and 0.595 ± 0.043 (Ehhalt et al., 1989; Sander et al., 2006; Talukdar et al., 1996) respectively. These processes enrich deuterium in atmospheric hydrogen, however they are not sufficient to explain the high deuterium content of tropospheric hydrogen, $\delta D(H_2)=120\pm4$‰ (Gerst and Quay, 2001; Rahn et al., 2003). Therefore it is necessary that atmospheric photochemical processes enrich D in hydrogen relative to the starting material to balance the isotope budget. The starting material is typically methane with a $\delta D(CH_4)$ value of -86 ± 3‰ (Quay et al., 1999), or isoprene, which is likely to be at least as depleted in D as methane (Feilberg et al., 2007). Isotopic analysis has been used to study hydrogen in the stratosphere which is confined to a small number of photochemicaly coupled species (mainly CH_4, H_2 and H_2O (McCarthy et al., 2004; Rhee et al., 2007)

It has recently been shown that HCDO is photolysed more slowly than HCHO, and that it produces less HD than HCHO produces H_2, (Feilberg et al., 2007) which would seem to contradict the observation that the process converting CH_4 to H_2 leads to deuterium enrichment (McCarthy et al., 2004; Rahn et al., 2003; Rockmann et al., 2003; Zahn et al., 2006). However the contradiction could be resolved if the depletion of deuterium in hydrogen produced by formaldehyde photolysis is offset by an even stronger enrichment in D in the steps producing formaldehyde. Unfortunately the isotope effects in this portion of the mechanism are not well-characterized. The relative rate of CH_3D vs. CH_4 oxidation is known, (Sander et al., 2006) but not the branching ratio for H vs. D abstraction from CH_3D. Atmospheric methyl radicals will be converted to methyl peroxy, which may react with NO to produce methoxy radicals. The formaldehyde and CO isotope effects have been described (Feilberg et al., 2004, 2005a, c, 2007; Weston, 2001). This paper addresses a key un-described reaction in the methane oxidation mechanism.

The title reaction (the numbering scheme of Table 1 will be used throughout)

$$CH_3O + O_2 \rightarrow HCHO + HO_2 \qquad \text{(R2)}$$

has been studied by several laboratories (Gutman et al., 1982; Lorenz et al., 1985; Wantuck et al., 1987) and the results have been analyzed and are available in kinetics compilations (Atkinson et al., 2006; NIST, 2007; Sander et al., 2006); $k_1=1.9\times10^{-15}$ cm^3 molecule^{-1} s^{-1} at 298 K. The Arrhenius A-factor, 3.9×10^{-14} cm^3 s^{-1} is low for a hydrogen atom transfer reaction indicating that the mechanism may be more complex than a simple abstraction (Sander, et al., 2006).

To improve understanding of hydrogen in the atmosphere we conducted a smog chamber FTIR study of the products of the $CH_2DO + O_2$ reaction. The results and a model of the photochemistry occurring in the reactor are presented herein and discussed with respect to the literature data and atmospheric implications.

2 Experimental and data analysis

2.1 FTIR-Smog chamber system at Ford

The experimental system used in this work has been described previously (Wallington and Japar, 1989) and is summarized here. The system is composed of a Pyrex tube with aluminum end flanges and has a volume of 140 L. The reactor was surrounded by 22 UV fluorescent lamps which were used to generate Cl via the photolysis of molecular chlorine. Experiments were performed at ambient temperature (295 ± 2 K) and a pressure of 930 ± 10 mbar of synthetic air. The concentrations of species in the photochemical reactor were determined using FTIR spectroscopy. The output beam of a Mattson Sirius 100 spectrometer was reflected through the reactor using White cell optics, giving an optical path length of 27 m. IR spectra at a resolution of 0.25 cm^{-1} were obtained by co-adding 32 interferograms. Unless stated, quoted uncertainties are two standard deviations derived from least-squares regressions.

2.2 Experimental procedure

CH_2DONO was synthesized by the drop-wise addition of concentrated sulfuric acid to a saturated solution of $NaNO_2$ in CH_2DOH (Cambridge Isotope Laboratories Inc., >98%) (Sokolov et al., 1999). CH_3ONO was synthesized analogously. The isotopic purity of the CH_2DONO was checked

Table 1. Reaction mechanism used to model methyl nitrite photolysis chemistry. The figure does not show the analogous monodeutero reactions and cross reactions; the full list of reactions and rates is available as supplementary information (http://www.atmos-chem-phys.net/7/5873/2007/acp-7-5873-2007-supplement.pdf). The mechanism was truncated by assuming in R28 that the peroxide has same reactivity as *c*-C_6H_{12}.

Reaction	Rate coefficient	Comments
R1. $CH_3ONO + h\nu \rightarrow CH_3O + NO$	1.44×10^{-3} s^{-1}	a
R2. $CH_3O + O_2 \rightarrow HCHO + HO_2$	1.9×10^{-15} cm^3 molecule^{-1} s^{-1}	b
R3. $HO_2 + NO \rightarrow OH + NO_2$	8.1×10^{-12} cm^3 molecule^{-1} s^{-1}	b
R4. $OH + cC_6H_{12} \rightarrow H_2O + RO_2$	6.37×10^{-12} cm^3 molecule^{-1} s^{-1}	c
R5. $RO_2 + NO \rightarrow RO + NO_2$	6.7×10^{-12} cm^3 molecule^{-1} s^{-1}	d
R6. $NO_2 + h\nu \rightarrow NO + O$	2.88×10^{-3} cm^3 molecule^{-1} s^{-1}	e
R7. $O + O_2 + M \rightarrow O_3 + M$	7.1×10^{-34} cm^6 molecule^{-2} s^{-1}	b
R8. $HCHO + h\nu \rightarrow CO + H_2$	5.5×10^{-5} s^{-1}	e, g
R9. $HCHO + h\nu \rightarrow CO + 2^*HO_2$	1.8×10^{-5} s^{-1}	e, g
R10. $HO_2 + NO_2 + M \rightarrow PNA + M$	1.8×10^{-31} cm^6 molecule^{-2} s^{-1}	b
R11. $HO_2 + HCHO \rightarrow HOCH_2O_2$	7.9×10^{-14} cm^3 molecule^{-1} s^{-1}	b, f
R12. $HOCH_2O_2 + RO_2 \rightarrow HCOOH + RO + HO_2$	5.0×10^{-14} cm^3 molecule^{-1} s^{-1}	h
R13. $CH_3O + NO + M \rightarrow CH_3ONO + M$	2.34×10^{-26} cm^6 molecule^{-2} s^{-1}	b
R14. $CH_3O + NO_2 + M \rightarrow CH_3ONO_2 + M$	5.46×10^{-26} cm^6 molecule^{-2} s^{-1}	b
R15. $OH + CH_3ONO \rightarrow HCHO + NO + H_2O$	3.0×10^{-13} cm^3 molecule^{-1} s^{-1}	b
R16. $HCHO + OH + O_2 \rightarrow H_2O + CO + HO_2$	8.5×10^{-12} cm^3 molecule^{-1} s^{-1}	b
R17. $HO_2 + HO_2 \rightarrow H_2O_2 + O_2$	1.7×10^{-12} cm^3 molecule^{-1} s^{-1}	b, f
R18. $H_2O_2 + h\nu \rightarrow 2OH$	5.47×10^{-6} molecule^{-1} s^{-1}	e
R19. $CH_3O + NO_2 \rightarrow HCHO + HONO$	2.0×10^{-13} cm^3 molecule^{-1} s^{-1}	b
R20. $2HOCH_2O_2 \rightarrow 2HCOOH + 2HO_2$	5.5×10^{-12} cm^3 molecule^{-1} s^{-1}	i
R21. $CH_3OH + OH \rightarrow CH_2OH + H_2O$	8.8×10^{-13} cm^3 molecule^{-1} s^{-1}	b
R22. $CH_2OH + O_2 \rightarrow HCHO + HO_2$	9.6×10^{-12} cm^3 molecule^{-1} s^{-1}	b
R23. $O_3 + NO \rightarrow NO_2 + O_2$	1.9×10^{-14} cm^3 molecule^{-1} s^{-1}	b
R24. $CO + OH + O_2 \rightarrow CO_2 + HO_2$	2.3×10^{-13} cm^3 molecule^{-1} s^{-1}	b, f
R25. $H_2 + OH \rightarrow H_2O + HO_2$	6.7×10^{-15} cm^3 molecule^{-1} s^{-1}	b
R26. $RO_2 + RO_2 \rightarrow 2RO$	1.3×10^{-14} cm^3 molecule^{-1} s^{-1}	j
R27. $RO_2 + RO_2 \rightarrow RO + cC_6H_{12}$	7.7×10^{-14} cm^3 molecule^{-1} s^{-1}	j
R28. $RO_2 + HO_2 \rightarrow cC_6H_{12}$ (recycle)	17.1×10^{-12} cm^3 molecule^{-1} s^{-1}	k
R29. $RO + O_2 \rightarrow cC_6H_{12} + HO_2$	2.0×10^{-17} cm^3 molecule^{-1} s^{-1}	h
R30a. $HOCH_2O_2 + HO_2 \rightarrow HOCH_2OOH + O_2$	6.0×10^{-12} cm^3 molecule^{-1} s^{-1}	h, l
R30b. $HOCH_2O_2 + HO_2 \rightarrow HCOOH + H_2O + O_2$	3.6×10^{-12} cm^3 molecule^{-1} s^{-1}	h, l
R30c. $HOCH_2O_2 + HO_2 \rightarrow HOCH_2O + OH + O_2$	2.4×10^{-12} cm^3 molecule^{-1} s^{-1}	h, l
R31. $NO_2 + OH + M \rightarrow HNO_3$	4.1×10^{-11} cm^3 molecule^{-1} s^{-1}	b, f
R32. $CH_3ONO_2 + OH \rightarrow HCHO + H_2O + NO_2$	3.0×10^{-13} cm^3 molecule^{-1} s^{-1}	b
R33. $HOCH_2O_2 \rightarrow HO_2 + HCHO$	150.0 s^{-1}	b
R34. $PNA \rightarrow HO_2 + NO_2$	10.0 s^{-1}	h

(a) This work.
(b) Rate coefficients from JPL (Sander, et al., 2006).
(c) (Wilson, et al., 2006)
(d) (Platz, et al., 1999)
(e) Photolysis rates calculated using estimated lamp flux curve and JPL cross sections photolysis rate relative to methyl nitrite.
(f) Based on JPL rate coefficient (Sander, et al., 2006), using pressure of reactor.

using IR spectroscopy which indicated an upper limit for a possible CH_3ONO impurity of 0.016%. Cyclohexane (ca. 100 ppm) was added to the reaction cell to limit unwanted reactions involving hydroxyl radicals. The concentration of cyclohexane in the initial reaction mixtures was about twice the concentration of methyl nitrite (ca. 50 ppm). During each experiment the reaction mixture was photolyzed in 5–7 steps, photolysis alternating with recording spectra,

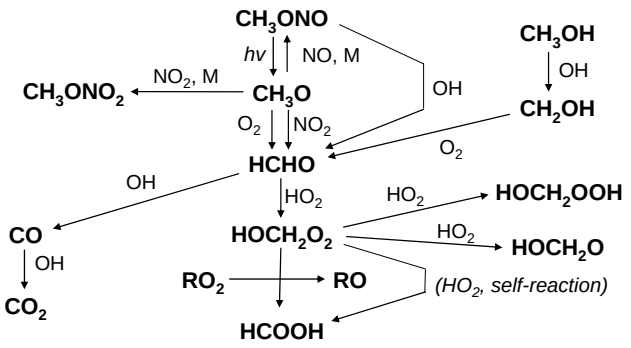

Fig. 2. Reactions of the carbon-containing species included in the model of reactor photochemistry. The figure does not show the analogous mono-deutero-reactions and cross reactions.

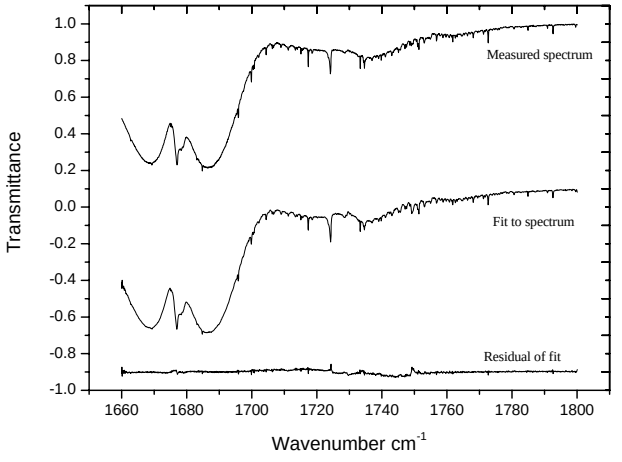

Fig. 3. Typical measured spectrum, fit to spectrum, and residual of fit after 20 s of photolysis. Compounds included in the fit are H_2O, N_2O, NO_2, HCHO, HCDO, CH_2DONO and HO_2NO_2. For clarity the spectra are offset vertically by 0, −0.9 and −0.9 units.

giving a total photolysis time of about 4 min. During a typical experiment 30% of the methyl nitrite was consumed and the final concentration of cyclohexane was >99% of the initial concentration.

The FTIR-spectra obtained from the experiments were analyzed using a nonlinear least squares spectral fitting procedure developed by Griffith (Griffith, 1996). Reference spectra for H_2O, N_2O and NO_2 were taken from the HITRAN database (Rothman et al., 2005). Absolute IR absorption cross sections for HCHO, HCDO and DCDO were measured in the LISA photochemical reactor at a resolution of $0.125\,cm^{-1}$, a path length of 12 m, a temperature of 296 K and a total pressure of 1013 mbar as detailed by Gratien et al. (2007a). The remaining reference spectra were recorded using conditions (temperature, total pressure in cell, path length, resolution) nominally identical to those used in the experiments.

2.3 Chemical model

A model of the chemistry occurring in the smog chamber using the CH_3ONO precursor was constructed using Maple (2005). The chemical mechanism is shown in Table 1 and Fig. 2, which omit the isotopic variants of the reactions for brevity; the 36 reactions shown here expand into 126 isotopic sub-reactions. The entire model and output are available as Electronic Supplementary Information (http://www.atmos-chem-phys.net/7/5873/2007/acp-7-5873-2007-supplement.pdf). Reaction rates were obtained from standard compilations when available, see Table 1 (Atkinson et al., 2006; NIST, 2007; Sander et al., 2006). Initial conditions were set using the nominal conditions of the reactor, in addition to photolysis rates based on the known performance of the lamps in past experiments. The main goal of the model was to investigate the possible role of sources of formaldehyde other than the title reaction, and to examine the potential magnitude of various loss mechanisms for formaldehyde including reactions with OH and HO_2, and photolysis.

3 Results and analysis

Figure 3 shows an example of the spectrum measured after 20 s of photolysis of the CH_2DONO precursor, the fit to the spectrum, and the residual. The measured spectrum is accurately reproduced by the fitting procedure. Compounds included in the fit are H_2O, N_2O, NO_2, HCHO, HCDO, CH_2DONO and HO_2NO_2. Spectral fitting becomes progressively more challenging as the experiment proceeds. Figure 4 shows the same series (experiment, fit, residual) after 4 min of photolysis. In addition to the compounds mentioned above, DCDO, HCOOH, DCOOD, DCOOH and CH_2DOH were included in the later fits. While the match between experiment and modeled spectrum is not as good as in Fig. 3, the overall shape and fine structure of the spectrum are fitted well, and from this we can conclude that all but trace components of the reaction mixture are accounted for. The region 1720–1750 cm^{-1} is the most important since this is where we see the $\nu(2)$ bands of HCHO and HCDO at 1746 and 1724 cm^{-1} respectively. It is likely that the larger residual in this region (compare Figs. 3 and 4) is due to the large number of species.

In all experiments, formic acid is present at concentrations comparable to those of HCHO. The relation between the concentrations of the formic acids appears to be [DCOOH] > [HCCOH] > [DCOOD], but this relation can not be quantatively verified due to the lack of calibrated reference spectra. DCDO is present at concentrations just slightly above the measurement threshold.

Figure 5 shows the results of the analysis, with the mole fraction of HCDO plotted versus that of HCHO. Results from three independent experiments are included in the figure. The

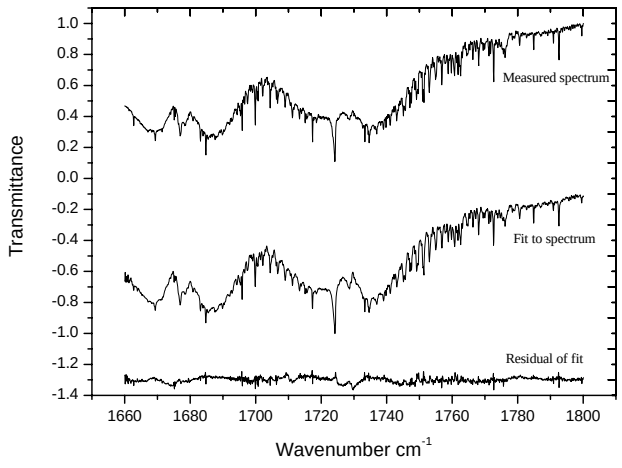

Fig. 4. Typical measured spectrum, fit to spectrum, and residual after 4 min of photolysis. Compounds included in the fit are the same as those in Fig. 3, plus DCDO, HCOOH, DCOOD, DCOOH and CH_2DOH. For clarity the spectra have been offset vertically by 0, −1.1, and −1.3 units, respectively.

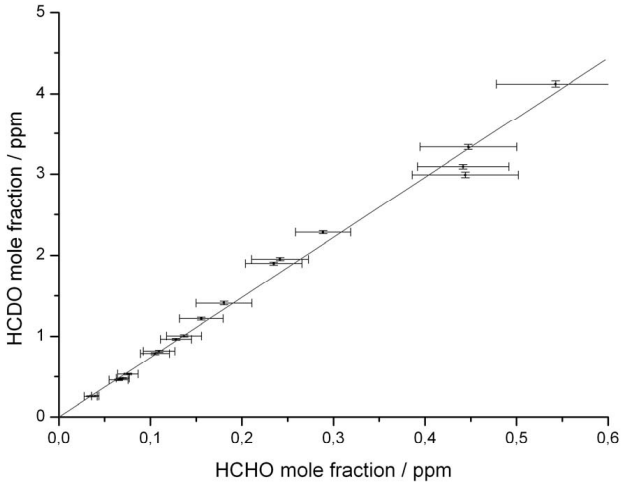

Fig. 5. The results of the analysis, with concentration of HCDO plotted versus concentration of HCHO. Results from three experiments are included in the figure. The slope of the line gives a branching ratio of 7.593±0.026.

fit to the data points, taking into account the statistical errors in the determinations of x_{HCDO} and x_{HCHO}, gives a relative rate k_{HCDO}/k_{HCHO} of 7.593±0.026 for production of HCDO vs. HCHO in the abstraction of H from CH_2DO by O_2.

The photochemistry of the precursor introduced competing sources of and loss processes for formaldehyde. The model showed a particular sensitivity to the isotopic purity of the CH_2DONO, since CH_3ONO would produce only HCHO, the minor product of $CH_2DO + O_2$. A spectrum of the CH_2DONO sample was recorded at relatively high pressure to look for traces of CH_3ONO, which were not seen. The previously determined upper limit of the concentration of CH_3ONO (0.016%) was used as a worst-case scenario in the model. The model showed that the title reaction is the dominant source of HCHO, accounting for >99.5% of the amount formed. The model shows that by the end of the experiment, 12% of the HCHO that is formed is lost via reaction with HO_2, and 4% by reaction with OH.

The methyl nitrite was synthesized from methanol and purified by distillation. As shown in Fig. 2 residual methanol is an alternative source of the formaldehyde isotopologues.

The model showed that 2.3% of the HCDO formed did not come from the CH_2DO precursor but instead reactions such as $CH_2DONO + OH \rightarrow HCDO + NO + H_2O$, $CHDOH + O_2$ and $CH_2DONO_2 + OH$. By the end of four minutes of photolysis 12% of the HCDO has been lost through reaction with HO_2, and 3% through reaction with OH. We are not aware of any reactions that would lead to isotopic scrambling of the hydrogen isotopes connected to the carbon atom.

The model was used to determine the branching ratio for HCDO vs. HCHO formed by the title reaction and without loss, as well as the actual concentration ratio of HCDO to HCHO that would be present in the cell. This indicated that the experimental branching ratio (7.293±0.026) should be decreased by ∼1.7%, which is insignificant compared to the other sources of error, discussed below. Even though some HCHO and HCDO is lost to reactions through the course of the experiment the model shows that this affects both formaldehyde isotopologues almost equally (i.e. in proportion to their concentration), thereby canceling when the relative rate is determined. Feilberg et al. (2004) have determined that the relative rate of reaction $k_{OH+HCHO}/k_{OH+HCDO}$ is 1.28±0.01 (Feilberg et al., 2004). The relative rate for the bimolecular combination reaction $k_{HO2+HCHO}/k_{HO2+HCDO}$ is not known but based on the mechanism only minor isotope effects are expected as D is a spectator. Nonetheless we assign a large uncertainty to the isotope effect of this reaction. In some cases when the reactivity of a deuterated species was not known a best estimate was made, for example the rate of H abstraction will scale with the number of H atoms, and a C–D bond's reactivity is 1/8 that of C–H, based on the reactivity of deuterated methanes. Since there is some unavoidable uncertainty in this process, it is reassuring that the model only indicated a minor correction; the final result is largely the direct result of the experiment and is rather insensitive to changes in the model.

The model takes advantage of earlier studies of the relative rate of reaction of the formaldehyde isotopologues with OH, (Feilberg et al., 2004) and of their relative photolysis rates and quantum yields (Feilberg et al., 2007) Sources of error in the experiment include the standard deviation of the measurement of the IR absorption cross sections of HCHO and HCDO, estimated to be 3% (Gratien et al., 2007a, b), and the error in the spectral fit shown in Fig. 5, 0.3%. The model

predicts that altogether 19% of HCHO and 17% of HCDO have been lost after 4 min of photolysis (and that this results in a 1.7% correction to the product ratio). An error of 50% in the amount of HCHO and HCDO lost was used to assess the overall error including for example uncertainty in the isotope effect of $k_{HO2+HCHO}/k_{HO2+HCDO}$. Altogether these considerations result in a relative rate of production of HCDO to HCHO of 7.46±0.76, or a branching ratio of 88.2±1.1% for HCDO and 11.8±1.1% for HCHO. The isotope effect is significant, given that on a purely statistical basis the corresponding numbers are 67%:33%.

A fraction of the formaldehydes is lost through reaction over the course of the experiment, mainly by reaction with OH and HO_2. These radicals cannot be observed directly, but their concentrations can be approximated using the model and the model can be checked for its ability to predict the concentrations of long-lived species. The reaction of OH with CH_2DONO is the main competing source of HCDO, producing <2.5% of the total. The source of OH is directly linked to methyl nitrite photolysis:

$$CH_3ONO + h\nu \rightarrow CH_3O + NO \quad \text{(R1)}$$

$$CH_3O + O_2 \rightarrow HCHO + HO_2 \quad \text{(R2)}$$

$$HO_2 + NO \rightarrow OH + NO_2 \quad \text{(R3)}$$

Cyclohexane was added to the cell to remove OH:

$$c - C_6H_{12} + OH \rightarrow R \cdot + H_2O \quad \text{(R4)}$$

The mechanism R1–R3 is straightforward, producing OH quantitatively when methyl nitrite is photolysed. In addition the lifetime of OH is controlled by R4 since cyclohexane is present in excess; according to the model over 95% of OH reacts with c-C_6H_{12}. According to the model the relative concentration of c-C_6H_{12} changes by $\sim 10^{-4}$ through the course of the experiment, maintaining a constant sink. Since the sources and sinks of OH are understood we feel that the model produces an accurate concentration, certainly within the 50% error assigned to the model correction.

According to the model over half of HO_2 is produced by R29, RO + O_2, and over 40% by the title reaction. These production rates are largely constant throughout the experiment. Over half of HO_2 reacts with NO via R3, and 1/3 produces HO_2NO_2(PNA) through R10. These rates are also relatively constant. HO_2 cycles between R11 and R20, converting formaldehyde into formic acid. One check that the model handles this reaction mechanism is shown in Fig. 6, the comparison between model and experimental formaldehyde concentrations.

Figure 6 also shows the carbon balance in the experiment and in the model. The fitting procedure can account for over 80% of the carbon in the experiment. One source of uncertainty is the lack of calibrated reference spectra for DCOOH, HCOOD and DCOOD; another is the estimated 3% error in the reference spectra for HCHO and HCDO.

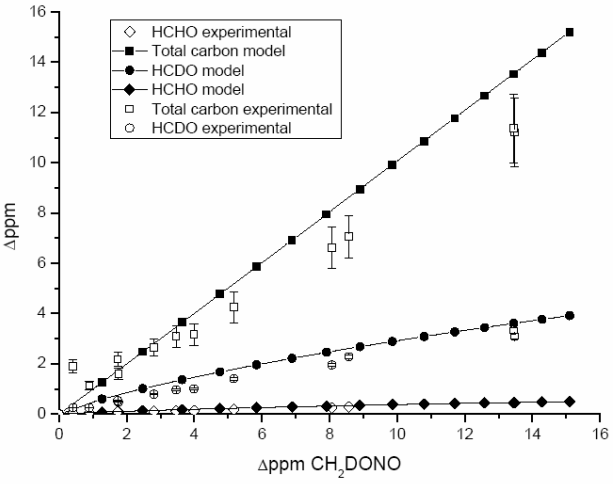

Fig. 6. Products yields predicted by the model (filled symbols) and those observed experimentally (open symbols).

The model provides insight into the reaction mechanism that would otherwise not be possible. The model supports the theory that a fraction of formaldehyde is lost by HOx reactions, and allows one to estimate what that fraction is. In addition the model demonstrates that alternative sources of formaldehyde are minor, and that the effect of side reactions on the branching ratio is minor.

4 Discussion

The greater activity of the H atom in methoxy towards abstraction by O_2, relative to D, leads to an enrichment in deuterium in atmospheric hydrogen. As shown in Feilberg et al. (2007) this enrichment is only partly counteracted by depletion in the photolysis of formaldehyde to produce molecular hydrogen and thus photochemically produced hydrogen is expected to be enriched in deuterium relative to the starting material, methane. This finding is in agreement with the results of field and modeling studies (Gerst and Quay, 2001; Keppler et al., 2006; Quay et al., 1999; Rhee et al., 2006b; Rockmann et al., 2003; Zahn et al., 2006). In addition the mechanistic detail provided can help in extending and refining the results of such studies.

Wantuck and coworkers, who investigated the absolute rate of the reaction in the range 298–973 K using laser induced fluorescence, distinguish three processes; simple hydrogen abstraction, isomerization ($CH_3O + O_2 \rightarrow CH_2OH + O_2$), and decomposition ($CH_3O + O_2 \rightarrow HCHO + H + O_2$) (Wantuck et al., 1987). The isomerization and decomposition processes explain the non-Arrhenius behavior at high temperature.

Setokuchi and Sato used variational transition state theory to derive the temperature dependence of the rate constant (Setokuchi and Sato, 2002), and the reaction mechanisms

have been examined in two studies (Bofill et al., 1999; Jungkamp and Seinfeld, 1996). Setokuchi and Sato report a theoretical rate constant of 9.9×10^{-16} cm^3 molecule^{-1} s^{-1} at 300 K, slightly below the experimental rate constant. Their work assumes that the reaction proceeds by direct hydrogen abstraction via a pre-reaction complex, as shown by Bofill et al. (1999). Three possible mechanisms are discussed by Bofill et al. (1999). The two more complicated mechanisms are disregarded since the activation energy is around 20 times higher than for the direct hydrogen abstraction reaction. The hydrogen abstraction reaction is predicted to have an activation energy of only 11.7 kJ/mol and an A-factor of 3.57×10^{-14} cm^3 molecule^{-1} s^{-1} at 298 K. These results are obtained from relative energies calculated at the RCCSD(T)/cc-pVTZ level and CASSCF/6-311G(d,p) level, using harmonic vibrational frequencies. Bofill et al. (1999) explained the small A-factor obtained in both computational and experimental studies in terms of a cyclic transition state (Bofill et al., 1999). According to the theoretical study by Bofill et al. (1999) the reaction of the methoxy radical with molecular oxygen occurs via direct hydrogen atom transfer, with a ring-like transition state (Bofill et al., 1999). The activation energy was determined to be 11.7 kJ mol^{-1} and when quantum tunneling was considered a rate constant was obtained that is in good agreement with the recommended experimental value. At room temperature hydrogen tunneling was the main route of reaction. This could explain the large value of the branching ratio in our study; hydrogen atoms, due to their lower mass, tunnel more easily than deuterium, thus leaving deuterium enriched on the carbon. The higher zero point energy of the C–H bond relative to C–D also plays a role.

The results of this study can be used in detailed models of tropospheric chemistry to investigate the carbon cycle. Several studies of deuterium make use of simplified chemical mechanisms (Rahn et al., 2003; Rhee et al., 2006a; Rockmann et al., 2003), however much remains to be learned, especially given the high variability of deuterium content in atmospheric formaldehyde. For example, a recent study by Rice and Quay found variation in δD(HCHO) between -296 and +210‰ for samples obtained in Seattle, Washington (Rice and Quay, 2006).

Acknowledgements. The authors wish to thank Niels Wessel Larsen, O. J. Nielsen and C. J. Nielsen for helpful discussions. M. S. Johnson and E. J. K. Nilsson thank the Copenhagen Center for Atmospheric Research supported by the Danish Natural Science Research Council and the Villum Kann Rasmussen Fund.

Edited by: R. Cox

References

Atkinson, R., Baulch, D. L., Cox, R. A., et al.: Evaluated kinetic and photochemical data for atmospheric chemistry: Volume II - gas phase reactions of organic species, Atmos. Chem. Phys., 6, 3625–4055, 2006.

Baroni, M., Thiemens, M. H., Delmas, J. H., and Savarino, J.: Mass-Independent Sulfur Isotopic Compositions in Stratospheric Volcanic Eruptions, Science, 315, 84–87, 2007.

Bofill, J. M., Olivella, J. M., Sole, A., and Anglada, J. M.: The mechanism of methoxy radical oxidation by O_2 in the gas phase. Computational evidence for direct H atom transfer assisted by an intermolecular noncovalent O··O bonding interaction, J. Am. Chem. Soc., 121, 1337–1347, 1999.

Boyd, A. A., Flaud, P. M., Daugey, N., and Lesclaux, R.: Rate constants for RO_2 + HO_2 reactions measured under a large excess of HO_2, J. Phys. Chem. A, 107, 818–821, 2003.

Brenninkmeijer, C. A. M., Janssen, C., Kaiser, J., et al.: Isotope effects in the chemistry of atmospheric trace compounds, Chem. Rev., 103, 5125–5161, 2003.

Ehhalt, D. H., Davidson, J. A., Cantrell, C. A., et al.: The Kinetic Isotope Effect in the Reaction of H_2 with OH, J. Geophys. Res.-Atmos., 94, 9831–9836, 1989.

Feilberg, K. L., D'Anna, B., Johnson, M. S., Nielsen, C. J., et al.: Relative tropospheric photolysis rates of HCHO, (HCHO)-C^{13}, (HCHO)-O^{18}, and DCDO measured at the European photoreactor facility, J. Phys. Chem. A, 109, 8314–8319, 2005a.

Feilberg, K. L., Griffith, D. W. T., Johnson, M. S., and Nielsen, C. J.: The C^{13} and D kinetic isotope effects in the reaction of CH_4 with Cl, Int. J. Chem. Kinet., 37, 110–118, 2005b.

Feilberg, K. L., Johnson, M. S., and Nielsen, C. J.: Relative reaction rates of HCHO, HCDO, DCDO, (HCHO)-C^{13}, and (HCHO)-O^{18} with OH, Cl, Br, and NO3 radicals, J. Phys. Chem. A, 108, 7393–7398, 2004.

Feilberg, K. L., Johnson, M. S., and Nielsen, C. J.: Relative rates of reaction of C^{13} O^{16}, C^{12} O^{18}, C^{12} O^{17} and C^{13} O^{18} with OH and OD radicals, Phys. Chem. Chem. Phys., 7, 2318–2323, 2005c.

Feilberg, K. L., Johnson, M. S., Bacak, A., et al.: Relative tropospheric photolysis rates of HCHO and HCDO measured at the European Photoreactor Facility, J. Phys. Chem. A, 111, 9034–9046, 2007.

Gerst, S. and Quay, P.: Deuterium component of the global molecular hydrogen cycle, J. Geophys. Res.-Atmos., 106, 5021–5031, 2001.

Gola, A. A., D'Anna, B., Feilberg, K. L., et al.: Kinetic isotope effects in the gas phase reactions of OH and Cl with CH_3Cl, CD_3Cl, and (CH_3Cl)-C^{13}, Atmos. Chem. and Phys., 5, 2395–2402, 2005.

Gratien, A., Nilsson, E., Doussin, J.-F., et al.: UV and IR absorption cross-sections of HCHO, HCDO and DCDO, J. Phys. Chem. A, 111, 11 506–11 513, 2007a.

Gratien, A., Picquet-Varrault, B., Orphal, J., et al.: Laboratory intercomparison of the formaldehyde absorption cross sections in the infrared (1660–1820 cm$^{(-1)}$) and ultraviolet (300–360 nm) spectral regions, J. Geophys. Res.-Atmos., 112, D05305, doi:10.1029/2006JD007201, 2007b.

Griffith, D. W. T.: Synthetic calibration and quantitative analysis of gas-phase FT-IR spectra, Appl. Spectrosc., 50, 59–70, 1996.

Gutman, D., Sander, N., and Butler, J. E.: Kinetics of the Reactions

of Methoxy and Ethoxy Radicals with Oxygen, J. Phys. Chem., 86, 66–70, 1982.

Hak, C., Pundt, I., Trick, S., et al.: Intercomparison of four different in-situ techniques for ambient formaldehyde measurements in urban air, Atmos. Chem. and Phys., 5, 2881–2900, 2005.

IPCC (2001), IPCC, Climate Change 2001: The Scientific Basis. Contribution of Working Group I to the Third Assessment Report of the Intergovernmental Panel on Climate Change, Cambridge University Press, New York.

Jenkin, M. E., Hurley, M. D., and Wallington, T. J.: Investigation of the radical product channel of the $CH_3C(O)O_2$+HO_2 reaction in the gas phase, Phys. Chem. Chem. Phys., 9, 3149–3162, 2007.

Johnson, M. S., Feilberg, K. L., von Hessberg, P., and Nielsen, O. J.: Isotopic processes in atmospheric chemistry, Chem. Soc. Rev., 31, 313–323, 2002.

Jungkamp, T. P. W. and Seinfeld, J. H.: The mechanism of methoxy radical oxidation: Hydrogen abstraction versus trioxy radical formation, Chem. Phys. Lett., 263, 371–378, 2002.

Keppler, F., Hamilton, J. T. G., Brass, M., and Rockmann, T.: Methane emissions from terrestrial plants under aerobic conditions, Nature, 439, 187–191, 2006.

Keppler, F., Harper, D. B., Rockmann, T., et al.: New insight into the atmospheric chloromethane budget gained using stable carbon isotope ratios, Atmos. Chem. Phys., 5, 2403–2411, 2005.

Lorenz, K., Rhasa, D., Zellner, R., and Fritz, B.: Laser Photolysis - Lif Kinetic-Studies of the Reactions of CH_3O and CH_2CHO with O_2 between 300 K and 500 K, Ber. Bunsen Phys. Chem., 89, 341–342, 1985.

Maple: Maple 10, Waterloo Maple Inc., Maplesoft, 2005.

McCarthy, M. C., Boering, K. A., Rahn, T., et al.: The hydrogen isotopic composition of water vapor entering the stratosphere inferred from high-precision measurements of δCH_4 and δH_2, J. Geophys. Res.-Atmos., 109, D07304, doi:10.1029/2003JD004003, 2004.

Miller, J. B., Tans, P. P., White, J. W. C., et al.: The atmospheric signal of terrestrial carbon isotopic discrimination and its implication for partitioning carbon fluxes, Tellus B, 55, 197–206, 2003.

NIST: Chemical Kinetics Database on the Web, Standard Reference Database 17, Version 7.0 (Web Version), Release 1.4, http://kinetics.nist.gov/kinetics/index.jsp, 2007.

Palmer, P. I., Abbot, D. S., Fu, T. M., et al.: Quantifying the seasonal and interannual variability of North American isoprene emissions using satellite observations of the formaldehyde column, J. Geophys. Res.-Atmos., 111, D12315, doi:10.1029/2005JD006689, 2006.

Platz, J., Sehested, J., Nielsen, O. J., and Wallington, T. J.: Atmospheric chemistry of cyclohexane: UV spectra of c-C_6H_{11}· and (c-C_6H_{11})O_2(·) radicals, kinetics of the reactions of (c-C_6H_{11})O_2(·) radicals with NO and NO_2, and the fate of the alkoxy radical (c-C_6H_{11})O·, J. Phys. Chem. A, 103, 2688–2695, 1999.

Prather, M. J.: An environmental experiment with H_2?, Science, 302, 581–582, 2003.

Quay, P., Stutsman, J., Wilbur, D., et al.: The isotopic composition of atmospheric methane, Global. Biogeochem. Cy., 13, 445–461, 1999.

Rahn, T., Eiler, J. M., Boering, K. A., et al.: Extreme deuterium enrichment in stratospheric hydrogen and the global atmospheric budget of H_2, Nature, 424, 918–921, 2003.

Rhee, T. S., Brenninkmeijer, C. A. M., Brass, M., and Bruhl, C.: Isotopic composition of H_2 from CH_4 oxidation in the stratosphere and the troposphere, J. Geophys. Res.-Atmos., 111, D23303, doi:10.1029/2005JD006760, 2006a.

Rhee, T. S., Brenninkmeijer, C. A. M., and Rockmann, T.: The overwhelming role of soils in the global atmospheric hydrogen cycle, Atmos. Chem. Phys., 6, 1611–1625, 2006b.

Rhee, T. S., Brenninkmeijer, C. A. M., and Rockmann, T.: Hydrogen isotope fractionation in the photolysis of formaldehyde, Atmos. Chem. Phys. Discussions, 7, 12 715–12 750, 2007.

Rice, A. L. and Quay, P. D.: Isotopic analysis of atmospheric formaldehyde by gas chromatography isotope ratio mass spectrometry, Anal. Chem., 78, 6320–6326, 2006.

Rockmann, T., Jockel, P., Gros, V., et al.: Using C^{14}, C^{13}, O^{18} and O^{17} isotopic variations to provide insights into the high northern latitude surface CO inventory, Atmos. Chem. Phys., 2, 147–159, 2002.

Rockmann, T., Rhee, T. S., and Engel, A.: Heavy hydrogen in the stratosphere, Atmos. Chem. Phys., 3, 2015–2023, 2003.

Rothman, L. S., Jacquemart, D., Barbe, A., et al.: The HITRAN 2004 molecular spectroscopic database, J. Quant. Spectrosc. R. A., 96, 139–204, 2005.

Rowley, D. M., Lightfoot, P. D., Lesclaux, R., and Wallington, T. J.: Ultraviolet-Absorption Spectrum and Self-Reaction of Cyclopentylperoxy Radicals, J. Chem. Soc.-Faraday Transactions, 88, 1369–1376, 1992.

Sander, S. P., Friedl, R. R., Ravishankara, A. R., et al.: Chemical Kinetics and Photochemical Data for Use in Atmospheric Studies. Evaluation Number 15, National Aeronautics and Space Administration, Jet Propulsion Laboratory, California Institute of Technology, Pasadena, California.

Saueressig, G., Crowley, J. N., Bergamaschi, P., et al.: Carbon 13 and D kinetic isotope effects in the reactions of CH_4 with $O(^1D)$ and OH: New laboratory measurements and their implications for the isotopic composition of stratospheric methane, J. Geophys. Res.-Atmos., 106, 23 127–23 138, 2001.

Schultz, M. G., Diehl, T., Brasseur, G. P., and Zittel, W.: Air pollution and climate-forcing impacts of a global hydrogen economy, Science, 302, 624–627, 2003.

Setokuchi, O. and Sato, M.: Direct dynamics of an alkoxy radical (CH_3O, C_2H_5O, and i-C_3H_7O) reaction with an oxygen molecule, J. Phys. Chem. A, 106, 8124–8132, 2002.

Sokolov, O., Hurley, M. D., Ball, J. C., et al.: Kinetics of the reactions of chlorine atoms with CH_3ONO and CH_3ONO_2, Int. J. Chem. Kinet., 31, 357–359, 1999.

Talukdar, R. K., Gierczak, T., Goldfarb, L., et al.: Kinetics of hydroxyl radical reactions with isotopically labeled hydrogen, J. Phys. Chem., 100, 3037–3043, 1996.

Wallington, T. J. and Japar, S. M.: Fourier-Transform Infrared Kinetic-Studies of the Reaction of HONO with HNO_3, NO_3 and N_2O_5 at 295 K, J. Atmos. Chem., 9, 399–409, 1989.

Wang, Y. H. and Jacob, D. J.: Anthropogenic forcing on tropospheric ozone and OH since preindustrial times, J. Geophys. Res.-Atmos., 103, 31 123–31 135, 1998.

Wantuck, P. J., Oldenborg, R. C., Baughcum, S. L., and Winn, K. R.: Removal Rate-Constant Measurements for CH_3O by O_2 over the 298-973-K Range, J. Phys. Chem., 91, 4653–4655, 1987.

Weston, R. E.: Oxygen isotope effects in the oxidation of methane

to carbon monoxide, J. Phys. Chem. A, 105, 1656–1661, 2001.
Wilson, E. W., Hamilton, W. A., Kennington, H. R., et al.: Measurement and estimation of rate constants for the reactions of hydroxyl radical with several alkanes and cycloalkanes, J. Phys. Chem. A, 110, 3593–3604, 2006.
von Hessberg, P., Kaiser, j., Enghoff M., et al.: Ultra-violet absorption cross sections of isotopically substituted nitrous oxide species: (NNO)-N^{14}-N^{14}, (NNO)-N^{15}-N^{14}, (NNO)-N^{14}-N^{15} and (NNO)-N^{15}-N^{15}, Atmos. Chem. Phys., 4, 1237–1253, 2004.
Zahn, A., Franz, P., Bechtel, C., et al.: Modelling the budget of middle atmospheric water vapour isotopes, Atmos. Chem. Phys., 6, 2073–2090, 2006.